



Influence of solvent solubility parameter on the power law exponents and critical concentrations of one soluble polyimide in solution

Hongxiang Chen^{1,2} · Ensong Zhang³ · Xuemin Dai^{3,4} · Wenke Yang¹ · Xue Liu¹ · Xuepeng Qiu³ · Wei Liu¹ · Xiangling Ji¹

Received: 29 May 2018 / Accepted: 28 December 2018 / Published online: 16 January 2019
© The Polymer Society, Taipei 2019

Abstract

Solvent species influence the interactions of dissolved polymers in solution and consequently induce changes in solution properties. A soluble polyimide was synthesized through polycondensation, and four solvents, namely, *N,N*-dimethylacetamide (DMAc), *N*-methyl pyrrolidone (NMP), *N,N*-dimethylformamide (DMF), and dimethyl sulfoxide (DMSO), were selected to investigate systematically the influence of solubility parameter on solution power law behaviors. The power law relationship between specific viscosity and concentration was established using rheology and applying concepts from the Zimm, Rouse-Zimm, and Doi-Edwards models. All power law exponents were higher than theoretical predictions, and in the three concentration regions, i.e. dilute, semidilute unentangled, and semidilute entangled, the exponents increase, decrease, and increase, respectively, with respect to solubility parameter. Arguments derived from the listed models are proposed to explain these trends. The influences of solubility parameter on the overlap and entanglement concentrations are also discussed.

Keywords Polyimide · Solution property · Power law exponent · Critical concentration · Solubility parameter

Introduction

Polyimide (PI) is a high-performance polymer that has been widely used in aerospace, microelectronics, fire protection, and other fields in the form of resin, fiber, film, and foam

[1–9]. Generally, conventional PIs are hardly dissolved in most organic solvents due to their good chemical resistance properties. However, introducing flexible functional groups, such as fluoroalkyl group, in PI backbone can reduce the rigidity of the backbone and increase solubility without sacrificing its thermal and mechanical properties [10–12]. Thus, the solution behavior of soluble PIs has been studied. Wu and Siddiq synthesized two soluble PIs, studied the relationship between the *z*-average radius of gyration and weight-average molecular weight, and found that the two PIs exist as a slightly extended coil conformation in CHCl₃ [13]. Liu et al. synthesized two isomerized soluble PIs and studied their solution properties in DMF and THF with LiBr or tetrabutylammonium bromide. The power law exponents α and ν , which were evaluated from the equations $[\eta] = K_{\eta}M^{\alpha}$ and $R_g = K_gM^{\nu}$, are in the range of 0.66–0.67 and 0.55–0.56, respectively; these findings indicated that the PI chains exhibit random coil conformation, and the wormlike model suitably describes these chains in dilute solution due to local rigidity [14–16]. Savitski et al. studied the solution behavior of two soluble PIs, i.e., 6FDA-TFDB (see Scheme 1) and the fully aromatic HFBPDA-TFDB, and found that 6FDA-TFDB PI chain presents random coil conformation in dilute THF solution while HFBPDA-TFDB is more rigid [17]. Unfortunately, only few researchers have focused on

Electronic supplementary material The online version of this article (<https://doi.org/10.1007/s10965-018-1694-0>) contains supplementary material, which is available to authorized users.

✉ Wei Liu
wliu@ciac.ac.cn

✉ Xiangling Ji
xlji@ciac.ac.cn

¹ State Key Laboratory of Polymer Physics and Chemistry, Changchun Institute of Applied Chemistry, Chinese Academy of Sciences, Changchun 130022, People's Republic of China

² University of Science and Technology of China, Hefei 230026, People's Republic of China

³ Laboratory of Polymer Composites and Engineering, Changchun Institute of Applied Chemistry, Chinese Academy of Sciences, Changchun 130022, People's Republic of China

⁴ University of the Chinese Academy of Sciences, Beijing 100049, People's Republic of China

concentrated PI solution. Zhang et al. synthesized one fluorine-containing soluble PI sample, studied the power law behavior of viscosity vs. concentration from dilute solution to concentrated regime in DMF, and found that dipole–dipole interaction is a major factor causing the deviation of these exponents from neutral polymers [18]. They also investigated the influence of molecular weight on power law exponents and found that the system shows associating behavior for largely high molecular weight sample in DMF [19, 20]. In addition, they noticed that solvent quality affects the power law exponents markedly [18].

The effects of solvent feature on polymer solution properties have been reported in literature. Eom et al. analyzed the polyacrylonitrile (PAN) solutions in DMF and DMSO with different solubility parameters; they found that DMF with solubility parameter close to PAN can dissolve the sample faster than that of DMSO, but PAN/DMSO solutions are more homogeneous than DMF [21]. Li et al. demonstrated that solubility parameter not only influences the homogeneity of PAN solution but also the sol–gel transitions of concentrated PAN solutions [22]. Antonietti et al. studied the solution viscosity of polyelectrolyte–surfactant complexes in polar solvents (DMF, ethanol, and isopropanol), which exhibit polyelectrolyte behavior. They also applied modified Hess–Klein approach to describe the viscosity curves, which depend systematically on the dielectric constant of solvents [23]. Antoniou et al. selected water, formamide, DMSO, and ethanolamine solvents and investigated the influence of solvent properties on dextran conformation, including dipole moment, surface tension, empirical parameter of solvent polarity, and Hansen solubility parameters. They considered that hydrogen bonding is the most important contributor to the solubility of dextran in different solvents [24]. Thus, solvent features significantly influence the polymer solution properties.

The ratio of mixed DMF/THF solvent can affect the power law exponents [18]. To verify this hypothesis, herein, four kinds of solvents, namely, *N,N'*-dimethylacetamide (DMAc), *N*-methyl pyrrolidone (NMP), *N,N'*-dimethylformamide (DMF), and dimethylsulfoxide (DMSO), are selected to explore the influence of solubility parameter on the power law exponents and critical concentrations of one soluble 6FDA-TFDB PI. The Zimm model, Rouse–Zimm model, and Doi–Edwards model are applied in different concentration regions.

Experimental

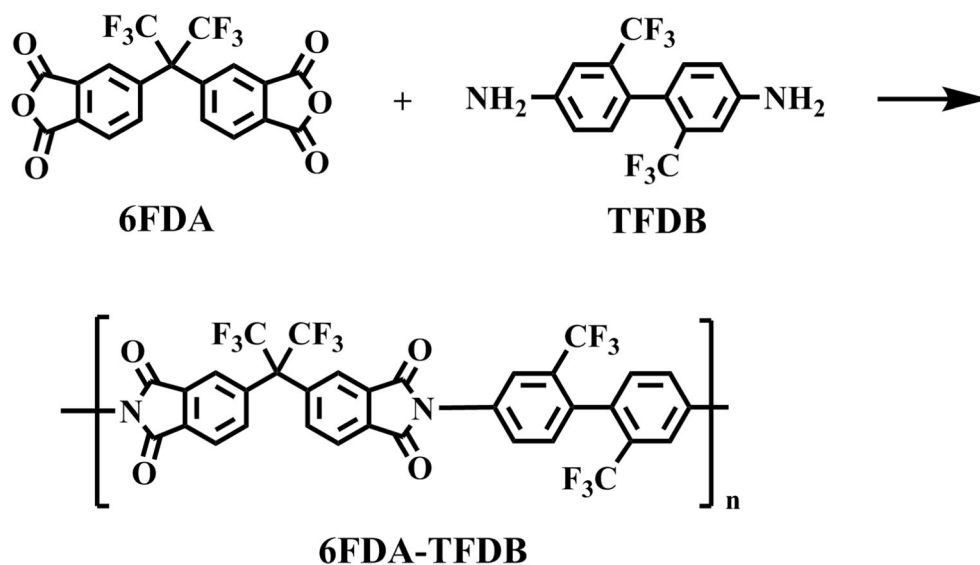
Chemicals

2,2'-Bis(trifluoromethyl)-4,4'-diaminobiphenyl (TFDB) and 2,2-bis(3,4-dicarboxyphenyl) hexafluoropropane dianhydride (6FDA), purchased from Beijing Multi Technology, was purified by sublimation in a vacuum at 130 °C and 250 °C for 48 h, respectively. *N,N'*-dimethylacetamide (DMA, anhydrous, 99.8%) was obtained from Sigma–Aldrich. Dimethylsulfoxide (DMSO), *N,N'*-dimethylformamide (DMF), *N*-methyl pyrrolidone (NMP), were purchased from Xilong Chemical Co. Ltd. with AR grade. DMSO was dried over molecular sieve beads (4 Å) and filtered through 0.22 μm filters. NMP was purified by distillation under reduced pressure after being dried overnight with CaH₂. Tetrabutylammonium bromide (TBAB, AR) was purchased from Sinopharm Chemical Reagent Co. Ltd.

Synthesis of polyamic acid solution

Under nitrogen atmosphere, 0.35 mol TFDB and 1600 mL DMAc were added in a 3 L three-necked flask with a stirring

Scheme 1 Synthetic procedure of 6FDA-TFDB polyimide sample



apparatus. After TFDB was dissolved completely, 0.35 mol 6FDA and moderate amount of *o*-phthalic anhydride were added into the flask. The mixture was stirred for 48 h at room temperature, and the dense polyamic acid solution was available.

Synthesis of polyimide (PI)

Chemical imidization reaction was last for 4 h to get PI solution after added 0.7 mol triethylamine and 1.4 mol acetic anhydride into the above polyamic acid solution. Methanol was used to precipitate the PI solution and then solid PI sample was available. In order to obtain thoroughly imidized polyimide, the above solid was put into a vacuum at 300 °C for 5 h. The synthetic procedure for 6FDA-TFDB polyimide was shown in Scheme 1.

Fractionation of PI sample

Typically, THF and water were served as good/poor solvent pair. In 3 L three-necked flask, 20 g PI sample was dissolved in 2000 mL THF to get approximately 1 wt% solution at room temperature. The solution was kept at least 24 h to equilibrium. Then appropriate amount of water was added to make the homogeneous solution turbid. After at least 24 h, the dense phase and dilute phase were separated by centrifuge. The dense phase was washed by water and dried in vacuum while the dilute phase was repeated the previous step for several times to get different fractions. Then, additional 140 g PI sample was fractionated through the same procedure. The obtained fractions were measured by size exclusion chromatography (SEC) to determine molecular weight and polydispersity index. The fractions with similar molecular weight were re-dissolved in THF and precipitated by water and dried in vacuum. At last, the fraction with narrow polydispersity index was available to carry out the following experiments.

Instruments and characterization

Fourier transform infrared (FTIR) spectra were recorded on a Bruker Vertex 70 spectrometer. ¹H NMR spectra were measured with a Bruker AV400 NMR spectrometer using DMSO-*d*₆ as a solvent. Size exclusion chromatography (SEC) coupled with multidetectors system, including a 515 pump (Waters Technologies), a 717 autosampler (Waters Technologies), two PL-gel 10 μm Mixed B-LS columns (Agilent Technologies), a ViscoStar Viscometer (Wyatt Technologies), a 2414 refractive index detector (Waters Technologies) and a DAWN HELEOS II multi-angle laser light scattering detector (MALLS) (Wyatt Technologies), was operated at 35 °C using DMF with 3.1 mmol TBAB as the mobile phase at a flow rate of 1 mL/min. Rheological measurements were performed using a TA instruments

DHR-2 stress-controlled rheometer with a cone plate geometry (40 mm in diameter, 2° cone plate geometry, 56 μm truncation). Peltier plate was used to control the temperature. Two semicircle 60 mm iron plates were covered around the plate geometry to prevent solvent evaporation.

Basic characterization of PI sample

The FT-IR spectrum of PI sample was shown in Fig. S1. The imide carbonyl group exhibited vibration at 1786 cm⁻¹ (C=O asymmetric stretching), 1728 cm⁻¹ (C=O symmetric stretching), 719 cm⁻¹ (C=O banding), and 1364 cm⁻¹ (C–N stretching). And amide groups near 3363 cm⁻¹ (N–H stretching) and 1650 cm⁻¹ (amide C=O strength) cannot be found, indicating a complete imidization. The ¹H NMR spectrum of PI in DMSO-*d*₆ was shown in Fig. S2. The resonance signals from different positions confirmed the related chemical structures of PI sample, which were as follows: δ 8.05 (d, J = 7.6 Hz, 2H), δ 7.94 (s, 2H), δ 7.87 (m, 4H), δ 7.68 (d, J = 8.2 Hz, 2H), and δ 7.44 (d, J = 8.2 Hz, 2H). The molecular weight distribution of pristine and experimental sample was displayed in Fig. S3. Based on the results of SEC coupled with multi-detectors, the absolute molecular weight *M*_w (SEC-MALLS) of experimental sample was 54,000 and PDI was 1.24.

Results and discussion

Solvent selection

Generally, the overall solubility parameter can be divided into three individual components, namely, dispersive force (δ_d), dipole interaction (δ_p), and hydrogen bonding (δ_h), i.e., δ² = δ_d² + δ_p² + δ_h². The overall solubility parameters of PI (6FDA-TFDB) calculated by Hoy's [25] and Fedor's method [26] are 24.0 and 24.6 J^{1/2} cm^{-3/2}, respectively. The average value of 24.3 J^{1/2} cm^{-3/2} is used in the present study, which is

Table 1 Overall and individual solubility parameters of solvents and PI (6FDA-TFDB)

Solvent	Solubility parameter (J ^{1/2} cm ^{-3/2})			
	δ	δ _d	δ _p	δ _h
DMAc	22.1	16.8	11.5	10.2
NMP	22.9	17.9	12.3	7.2
DMF	24.9	17.4	13.7	11.3
DMSO	26.5	18.4	16.4	10.2
PI ^a	24.3	20.0	13.3	3.9

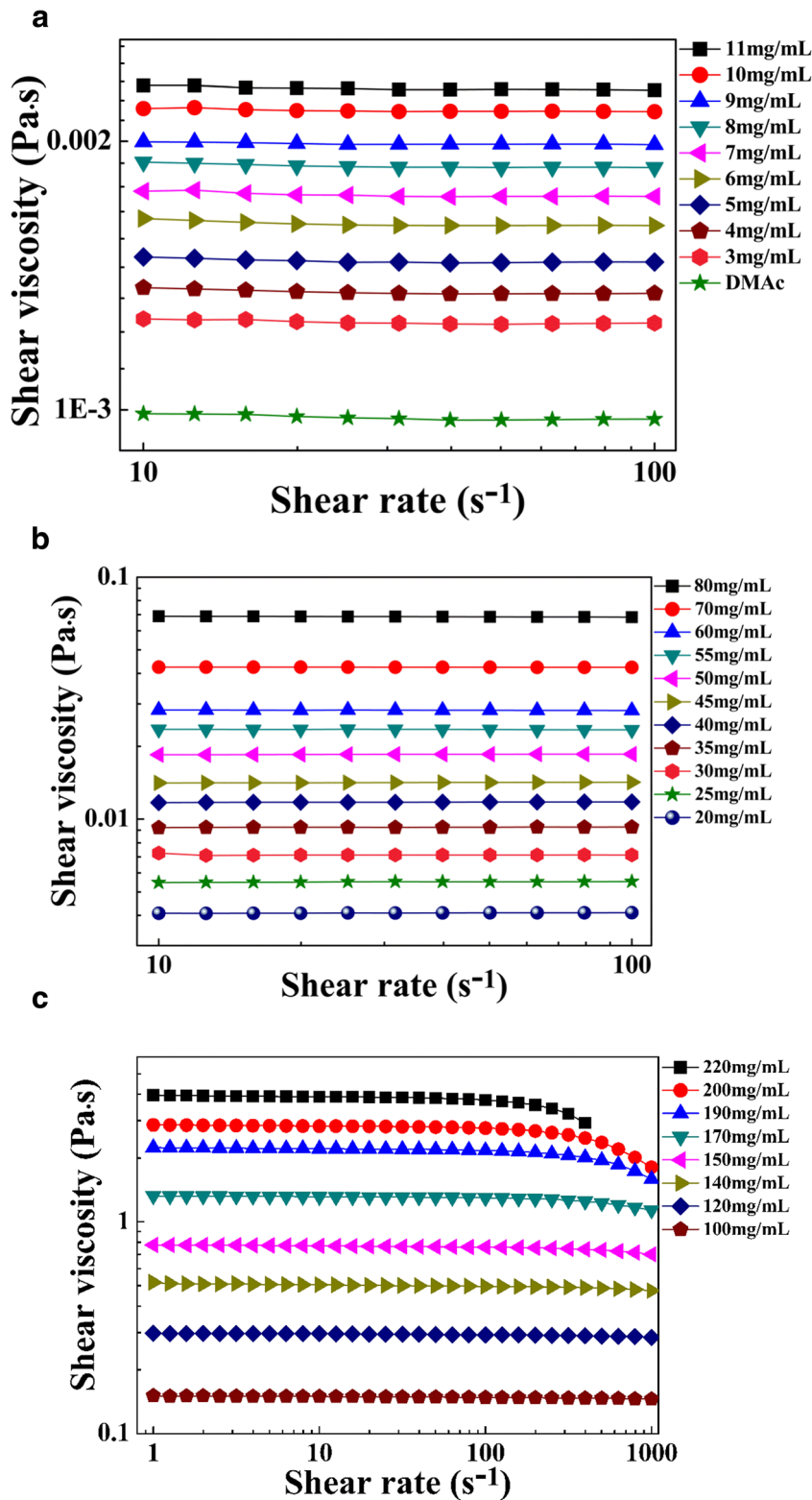
^a Calculated from Hoy's and Fedor's method [25, 26]

similar to that reported by Savitski [17]. The individual solubility parameters are calculated by using Hoy's method.

Finally, DMAc, NMP, DMF, and DMSO with solubility parameters of 22.1, 22.9, 24.9, and 26.5 $J^{1/2} cm^{-3/2}$

respectively, are selected for the experiment. The overall and individual solubility parameters of the different solvents and PI sample are listed in Table 1.

Fig. 1 Shear viscosity against shear rate for of 6FDA-TFDB PI/DMAc solutions with different concentrations at 20 °C, **a** 0–11 mg/mL **b** 20–70 mg/mL **c** 100–220 mg/mL



Flow curves of different solutions at different concentrations

The variation in the viscosity of PI/DMAc solutions at different concentrations (0–220 mg/mL) under 20 °C is shown in Fig. 1. The zero shear viscosity of PI/DMAc solutions increases gradually from 9.76×10^{-4} Pa·s to 3.96 Pa·s, while the concentration increases from 0 mg/mL to 220 mg/mL. All solutions display Newtonian behavior (linear region) at low shear rate. When the concentration reaches 100 mg/mL, shear thinning is observed at higher shear rate. And the critical shear rate, where the onset of shear thinning occurs, decreases with increased concentration.

The flow curves for PI/DMAc solution at 25 °C, 30 °C, 35 °C, 40 °C, and 45 °C are shown in Figures S4–S8. The flow curves for PI/NMP, PI/DMF, and PI/DMSO solution at 20 °C, 25 °C, 30 °C, 35 °C, 40 °C, and 45 °C are presented in Figures S9–S26. Similar trend can be found in Figures S4–S26.

Power law relationship in different concentration regions and critical concentrations

Herein, three concentration regions, i.e., dilute solution, semidilute unentangled solution, and semidilute entangled solution, are discussed.

In dilute solution, polymer chains acts as separated coils and Zimm model is suitable in this situation. The polymer chain is represented as N beads connected by $N - 1$ springs (bead-spring model). Then the relation of viscosity versus concentration can be expressed as follows [27]:

$$\eta - \eta_s = \int_0^\infty G(t) dt \approx \frac{kT}{b^3} \phi \int_0^\infty \left(\frac{t}{\tau_0}\right)^{-\frac{1}{3\nu}} \exp\left(-\frac{t}{\tau_z}\right) dt$$

$$\approx \frac{kT}{b^3} \phi \tau_z \left(\frac{\tau_z}{\tau_0}\right)^{-\frac{1}{3\nu}} \int_0^\infty x^{-\frac{1}{3\nu}} \exp(-x) dx \approx \frac{kT}{b^3} \phi \tau_0 N^{3\nu-1} \approx \eta_s \phi N^{3\nu-1}$$

(1)

In semidilute unentangled solution, a hydrodynamic screen length exists. On length scales shorter than the length, the hydrodynamic interaction domains and the Zimm model is suitable. When length scales are larger than the length, the hydrodynamic interaction is screened by the surrounding chains and Rouse model can be used to describe the relaxation time τ_{chain} . Finally, the relation of viscosity versus concentration can be expressed as follows:

$$\eta - \eta_s = \int_0^\infty G(t) dt \approx \frac{kT}{b^3} \frac{\phi}{N} \tau_{chain} \approx \eta_s N \phi^{1/(3\nu-1)}$$

(2)

In semidilute entangled solutions, the Edwards tube model was used to describe the entangled polymer dynamics [28]. Here exists a dynamic length scale called Edwards tube

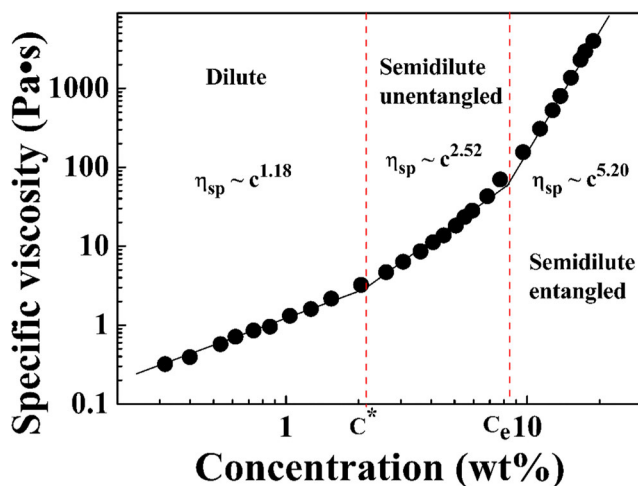


Fig. 2 Power law relationship between specific viscosity and concentration for 6FDA-TFDB PI/DMAc solution at 20 °C

diameter α . The relaxation time outside the Edwards tube diameter τ_{rep} can be determined using Edwards tube model [29]. Finally, the relation of viscosity versus concentration can be expressed as follows:

$$\eta - \eta_s \approx G_e \tau_{rep} \approx \eta_s \frac{N^3}{[N_e(1)]^2} \begin{cases} \phi^{3/(3\nu-1)} & (\text{athermal solvent}) \\ \phi^{14/3} & (\theta\text{-solvent}) \end{cases}$$

(3)

In the current work, zero shear viscosity (η_0) is used to estimate the specific viscosity (η_{sp}). In dilute and semidilute unentangled solutions, the Newtonian plateau viscosity is considered as η_0 . In the semidilute entangled region, η_0 can be determined by the Carreau model [30].

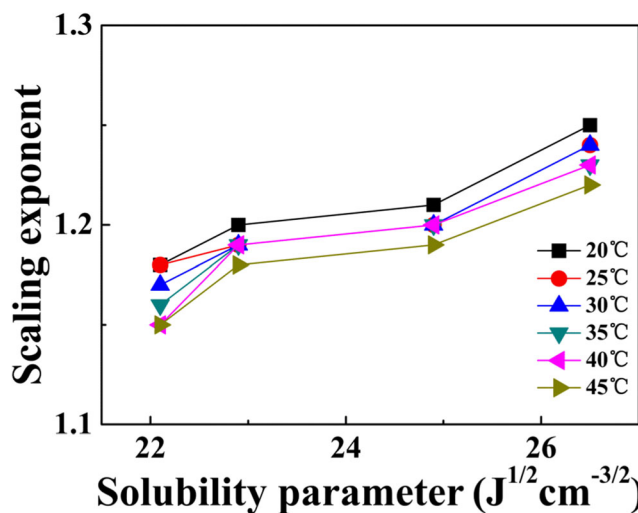


Fig. 3 Variation of power law exponent with solvent solubility parameter for PI sample in dilute solution at different temperatures

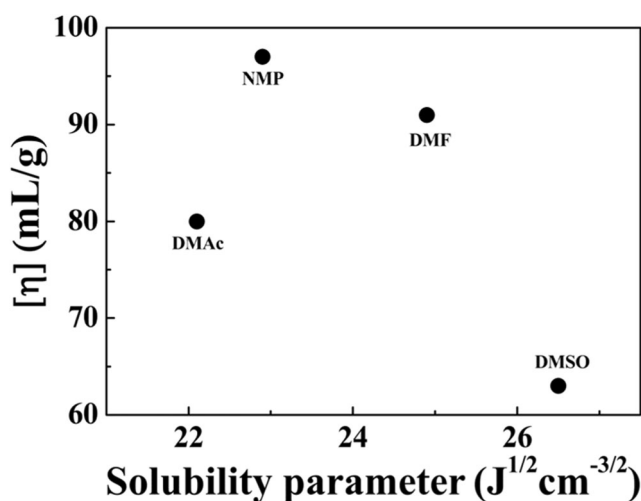
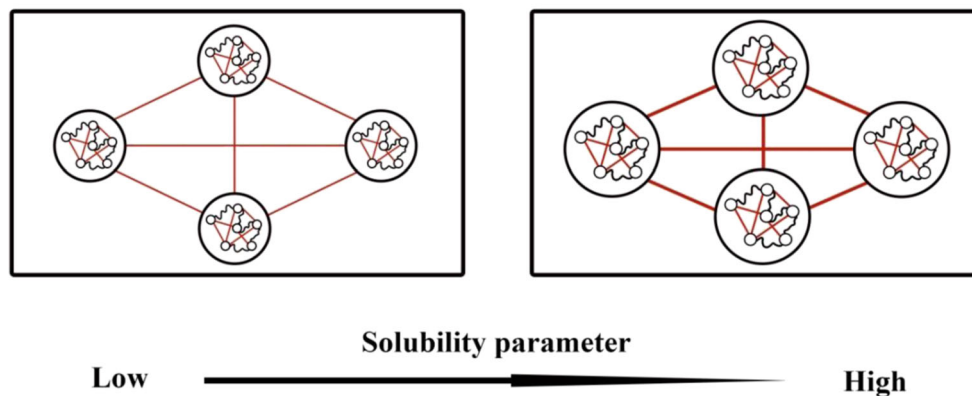
Table 2 Power law exponents in different solvents at different temperatures in dilute solution

Solvent	20 °C	25 °C	30 °C	35 °C	40 °C	45 °C
DMAc	1.18 ± 0.02	1.18 ± 0.03	1.17 ± 0.03	1.16 ± 0.03	1.15 ± 0.03	1.15 ± 0.05
NMP	1.20 ± 0.02	1.19 ± 0.02	1.19 ± 0.02	1.19 ± 0.02	1.19 ± 0.02	1.18 ± 0.02
DMF	1.21 ± 0.03	1.20 ± 0.04	1.20 ± 0.04	1.20 ± 0.05	1.20 ± 0.05	1.19 ± 0.06
DMSO	1.25 ± 0.02	1.24 ± 0.02	1.24 ± 0.02	1.23 ± 0.02	1.23 ± 0.02	1.22 ± 0.02

$$\eta = \frac{\eta_0}{[1 + (\lambda\dot{\gamma})^2]^{\frac{1-n}{2}}} \quad (4)$$

where η_0 is zero shear viscosity, λ is the relaxation time, $\dot{\gamma}$ is the shear rate, and n is the exponent of power law.

A typical relationship between specific viscosity $\eta_{sp} = (\eta - \eta_s)/\eta_s$ and concentration in DMAc solution at 20 °C is established as shown in Fig. 2. The relationships in DMF, NMP, and DMSO solutions are shown in Figures S27–S29.

**Fig. 4** Intrinsic viscosity of 6FDA-TFDB PI sample in different solvents at 20 °C**Fig. 5** Proposed model for polyimide chains in different solvents in dilute solution

The power law exponents between specific viscosity (η_{sp}) and concentration can be obtained in three concentration regions:

$$\begin{aligned} \eta_{sp} &\sim C^{1.18 \pm 0.02} && \text{in dilute solution} \\ \eta_{sp} &\sim C^{2.52 \pm 0.08} && \text{in semidilute unentangled solution} \\ \eta_{sp} &\sim C^{5.20 \pm 0.10} && \text{in semidilute entangled solution} \end{aligned}$$

The theoretical power law exponents for polymers in θ (good) solvent are 1.0 (1.0), 2.0 (1.3), and $14/3 \approx 4.67$ (3.9) in dilute, semidilute unentangled, and semidilute entangled solutions, respectively [31].

The power law exponents are 1.18, 2.52, and 5.20, which correspond to dilute, semidilute unentangled, and semidilute entangled solutions, respectively, for PI/DMAc solution at 20 °C. All the power law exponents are higher than the theoretical values, which is similar to Zhang's results [18, 19].

The overlap concentration (C^*) and entanglement concentration (C_e) are also available. C^* is 2.7 wt%, and C_e is 8.6 wt% for PI/DMAc at 20 °C.

Influence of solvent solubility parameter on power law exponent in dilute solution

According to theoretical prediction, the power law exponent, which is obtained from the relationship between specific viscosity and concentration, is 1.0 for neutral polymer in dilute solutions [28, 32, 33], such as cellulose 1-ethyl-3-methylimidazolium acetate solutions. The variation of power

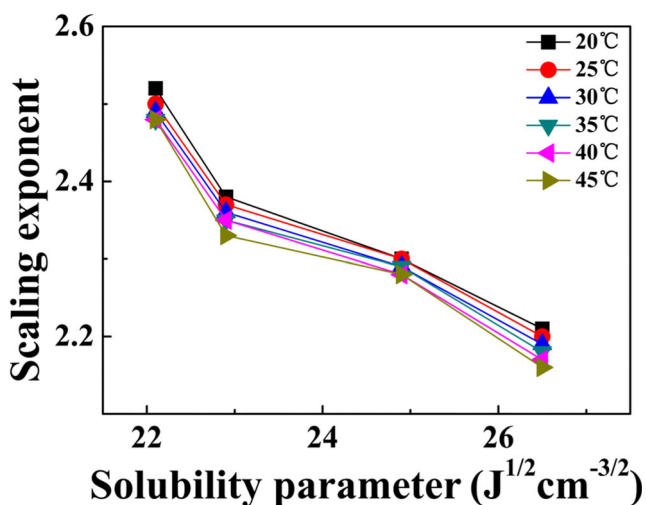


Fig. 6 Relationship between power law exponent and solubility parameter for 6FDA-TFDB PI sample in semidilute unentangled solution at different temperatures

law exponent with solvent solubility parameters at different temperatures in dilute solution is shown in Fig. 3. The details are listed in Table 2. At 20 °C, the power law exponents are 1.18, 1.20, 1.21, and 1.25 in DMAc, NMP, DMF, and DMSO, respectively. All the power law exponents are higher than the theoretical values and these values are rather close at various temperatures. Zhang reported that the deviation of power law exponents in dilute solution is due to the interaction between polymer coils [18]. In infinite dilute concentration region, each polymer chain can be considered a random coil with a hydrodynamic volume. These coils separate apart and can't feel each other. The radius of polymer coils can be affected by solvent type, which is shown in Fig. 4. The $[\eta]$ values of these solutions are determined from the Huggins and Kraemer equations [34, 35], which are 80, 97, 91, and 63 mL/g at 20 °C in DMAc, NMP, DMF, and DMSO, respectively, following the order NMP > DMF > DMAc > DMSO. We believe that the concentration exponent is exactly 1.0 in infinite dilute solution. As concentration increases, the possibility that polymer coils interact with each other increase. This interaction is the main factor causing the power law exponents higher than 1.0. The power law exponents increase with solubility parameter in this concentration region. As shown in Fig. 5, a model is proposed to understand the results in solvents with different solubility parameters.

Solvents with different solubility parameters exhibit different powers in screening dipole–dipole interaction, thereby influencing the polymer coil radius. Among the four solvents, DMSO demonstrates the highest solubility parameter, which represents the high polarity of solvent. DMSO can screen the intrachain interaction and extend the polymer chain, which means an increased possibility to contact each other between polymer coils in dilute solution. Thus, the deviation in power law exponent is the highest in PI/DMSO solution. On the contrary, the deviation in power law exponent is the lowest in PI/DMAc solution.

As shown in Table 2, the power law exponents are 1.18, 1.18, 1.17, 1.16, 1.15, and 1.15 when the temperature increases from 20 °C to 45 °C. This result shows slightly decreased trend with increased temperature. The conformational entropy plays a larger role at higher temperature, which means the interaction between polymer coils becomes weaker. Additionally, increased temperature makes solvent better for PI, which indicates the increase in polymer coil radius. These reasons result in slightly decreased power law exponents with increased temperature.

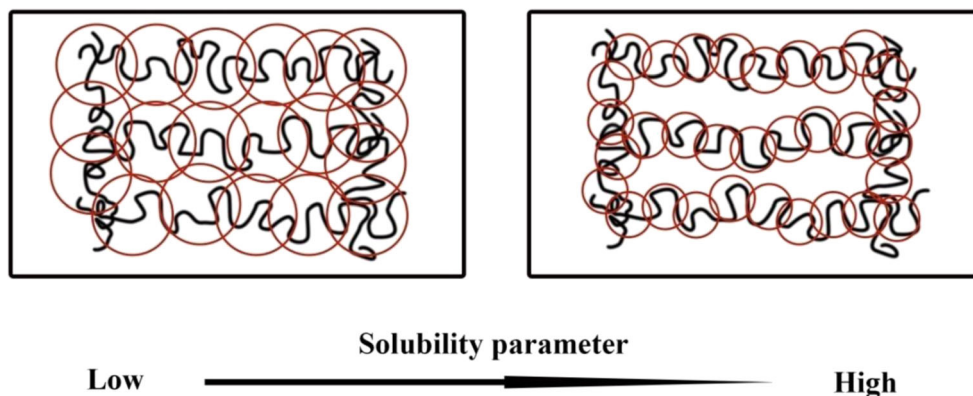
Influence of solvent solubility parameter on power law exponent in semidilute unentangled solution

According to theoretical prediction, the power law exponent is 1.3 (good solvent)–2.0 (θ solvent) for neutral polymer in semidilute unentangled solution [28, 32, 33]. The variation in power law exponent with solubility parameters at different temperatures in semidilute unentangled solution is shown in Fig. 6. Results are also listed in Table 3. At 20 °C, power law exponents are 2.52, 2.38, 2.30, and 2.21 in DMAc, NMP, DMF, and DMSO, respectively, and the corresponding solubility parameters increase from 22.1 $J^{1/2} cm^{-3/2}$ to 26.5 $J^{1/2} cm^{-3/2}$. Under other temperatures, power law exponents exhibit the same trend with solvent solubility parameter. At 45 °C, the power law exponents are 2.48, 2.33, 2.28, and 2.16 in DMAc, NMP, DMF, and DMSO, respectively. Notably, all the power law exponents are higher than the theoretical value (1.3–2.0). In semidilute unentangled region, the polymer coils overlap, and the Zimm and Rouse models suitably describe the inside and outside of a blob, respectively. In previous work, the deviation of power law exponents in

Table 3 Power law exponents in different solvents at different temperatures in semidilute unentangled solution

Solvent	20 °C	25 °C	30 °C	35 °C	40 °C	45 °C
DMAc	2.52 ± 0.08	2.50 ± 0.08	2.49 ± 0.09	2.48 ± 0.09	2.48 ± 0.09	2.48 ± 0.09
NMP	2.38 ± 0.06	2.37 ± 0.06	2.36 ± 0.06	2.35 ± 0.06	2.35 ± 0.06	2.33 ± 0.06
DMF	2.30 ± 0.05	2.30 ± 0.05	2.29 ± 0.05	2.29 ± 0.05	2.28 ± 0.05	2.28 ± 0.06
DMSO	2.21 ± 0.08	2.22 ± 0.08	2.19 ± 0.08	2.18 ± 0.08	2.17 ± 0.08	2.16 ± 0.08

Fig. 7 Proposed model for polyimide chains in semidilute unentangled solution



6FDA-TFDB PI/DMF solution is mainly due to the dipole-dipole interactions from interchain segments and π - π stacking, which are also called the relatively weak interactions [18]. A model is proposed in Fig. 7. Given the effects of solvent on the interaction between chain segments, the use of effective weak interaction space indicated in the red circle explains the presented results. When the red circles overlap, the weak interaction between chain segments causes an increase in the power law exponent. When the solvent solubility parameter increases, the scale of the effective weak interaction space decreases. The overlapping area also decreases, which weakens the interaction between chain segments. Thus, the power law exponent shows a decreased trend with solubility parameters.

The power law exponents decrease with temperature, which is demonstrated in Fig. 6 and Table 3. For example, the power law exponents in DMAc are 2.52, 2.50, 2.49, 2.48, 2.48, and 2.48 when the temperature increases from 20 °C to 45 °C. When the polymer concentration exceeds overlap concentration, the interactions between chains become dominant. In the Zimm-Rouse model, the specific viscosity in semidilute unentangled solution can be expressed as in Eq. (2). With increased temperature, solvents become better for PI (increased ν), leading to the decrease of the power law exponents. The conformational entropy plays a larger role at higher temperature, which means the interaction between polymer segments becomes weaker. Thus, the power law exponent decreases with increased temperature.

Influence of solvent solubility parameter on power law exponent in semidilute entangled solution

The theoretical power law exponent is in the range of 3.9 (good solvent)–4.67 (θ solvent) for neutral polymer in semidilute entangled solution [28, 32, 33]. The variation in power law exponents with solvent solubility parameters at different temperatures in semidilute entangled solution is shown in Fig. 8. The details are also listed in Table 4. At 20 °C, the power law exponent increases from 5.20 (in DMAc) to 5.65 (in DMSO) when the solubility parameter

changes from $22.1 \text{ J}^{1/2} \text{ cm}^{-3/2}$ to $26.5 \text{ J}^{1/2} \text{ cm}^{-3/2}$. The power law exponents follow the same trend at 25 °C–45 °C. All the power law exponents are much higher than the theoretical value. In semidilute entangled solution, the polymer chains topologically constrain and entangle with one another, and the Doi-Edwards tube model suitably describes this case [28]. PI segments interact with the “tube” formed by surrounding chains, which inhibits the reptation of PI chain from the “tube”. And this is the main factor causing the deviation in the power law exponent in semidilute entangled solution [18]. As shown in Fig. 9, the relatively weak interaction (i.e., dipole-dipole and π - π interactions) space (red circle) interacts with the “tube”. When the radius of the red circles overlaps with the “tube” radius, the interaction between the PI segments and the “tube” is eliminated. When the solvent solubility parameter increases, the scale of the relatively weak interaction space decreases. Consequently, the interaction between the chain segments and the “tube” is enhanced, which inhibits the reptation of PI chain from the tube, thereby increasing the power law exponents.

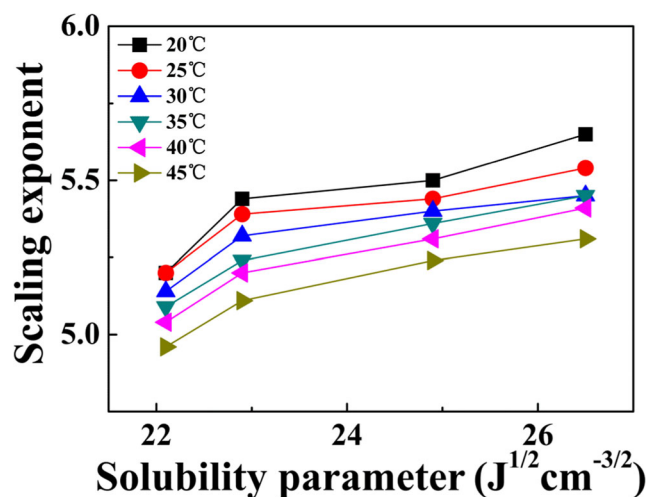


Fig. 8 Relationship between power law exponent and solubility parameter for 6FDA-TFDB PI sample in semidilute entangled solution at different temperatures

Table 4 Power law exponents in different solvents at different temperatures in semidilute entangled solution

Solvent	20 °C	25 °C	30 °C	35 °C	40 °C	45 °C
DMAc	5.20 ± 0.10	5.20 ± 0.08	5.14 ± 0.07	5.09 ± 0.06	5.04 ± 0.06	4.96 ± 0.06
NMP	5.44 ± 0.11	5.39 ± 0.11	5.32 ± 0.11	5.24 ± 0.11	5.20 ± 0.12	5.11 ± 0.11
DMF	5.50 ± 0.07	5.44 ± 0.09	5.40 ± 0.09	5.36 ± 0.10	5.31 ± 0.10	5.24 ± 0.10
DMSO	5.65 ± 0.11	5.54 ± 0.14	5.45 ± 0.13	5.45 ± 0.13	5.41 ± 0.14	5.31 ± 0.10

In Fig. 8 and Table 4, the power law exponents decrease with increased temperature in semidilute entangled solution. For example, the power law exponents in DMAc are 5.20, 5.20, 5.14, 5.09, 5.04, and 4.96 when the temperature increases from 20 °C to 45 °C. When the concentration of polymer solutions is above the entanglement concentration, the specific viscosity can be expressed as in Eq. (3). When the temperature increases, solvents become better for PI (increased ν), leading to the decrease of the power law exponents. The conformational entropy plays a larger role at higher temperature, which means the interaction between chain segments and the “tube” becomes weaker. Thus, the power law exponent decreases with increased temperature.

Influence of solvent solubility parameter on overlap concentration (C*) and entanglement concentration (C_e)

The variation in overlap concentration with solvent solubility parameter at different temperatures is shown in Fig. 10. At 20 °C, the C* values are 2.7 wt%, 2.2 wt%, 2.0 wt%, and 1.7 wt% when the solubility parameters are 22.1, 22.9, 24.9, and 26.5 J^{1/2} cm^{-3/2}, respectively. The details are listed in Table 5. The overlap concentration decreases with increased solubility parameter. Solvents with different solubility parameters exhibit different powers in screening dipole–dipole interaction. Thus, polymer coil radius changes with solubility parameter. Solvent with high polarity can screen the intrachain interaction effectively and extend the polymer chain, which means the increased possibility to contact each other between

polymer coils. Thus, the overlap concentration decreases with increased solubility parameter. As shown in Fig. 10 and Table 5, the C* in different solvent decreases slightly with decreasing temperature. Increased temperature can make the solvent become better, and increase the polymer coil radius, which increases the possibility for polymer chain to contact with each other. Thus, the overlap concentration decreases with increased temperature.

The variation in the entanglement concentration (C_e) with solubility parameter at different temperatures is illustrated in Fig. 11. The detailed results are listed in Table 6. At 20 °C, the C_e values are 8.6 wt%, 8.0 wt%, 8.1 wt%, and 7.3 wt%, which correspond to the solubility parameters of 22.1, 22.9, 24.9, and 26.5 J^{1/2} cm^{-3/2}, respectively. At 40 °C, the corresponding C_e values are 8.5 wt%, 8.1 wt%, 8.0 wt%, and 7.2 wt%. Evidently, C_e decreases with solvent solubility parameter. The larger radius of PI chains also suggests increased possibility of entanglement. Therefore, the entanglement concentration decreases with increased solubility parameter. Increasing temperature also increases the radius of polymer coils and the possibility for polymer chains to contact with each other. Thus, C_e also decreases with increased temperature.

Conclusions

DMAc, NMP, DMF, and DMSO are selected to investigate the influence of solvent solubility parameter on power law exponents and critical concentrations at 20 °C–45 °C in 6FDA-

Semidilute entangled

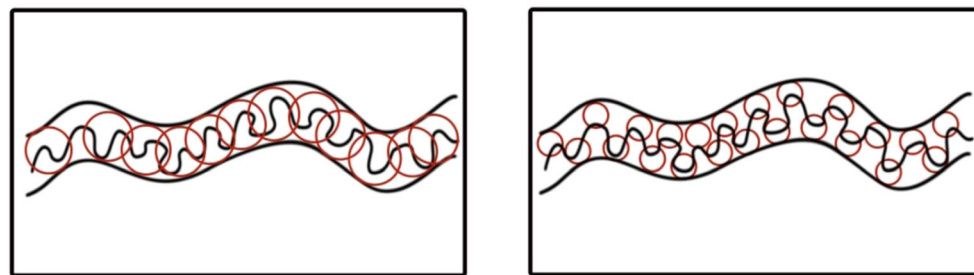


Fig. 9 Proposed model for polyimide chains in semidilute entangled solution

Low ————— Solubility parameter ————— High

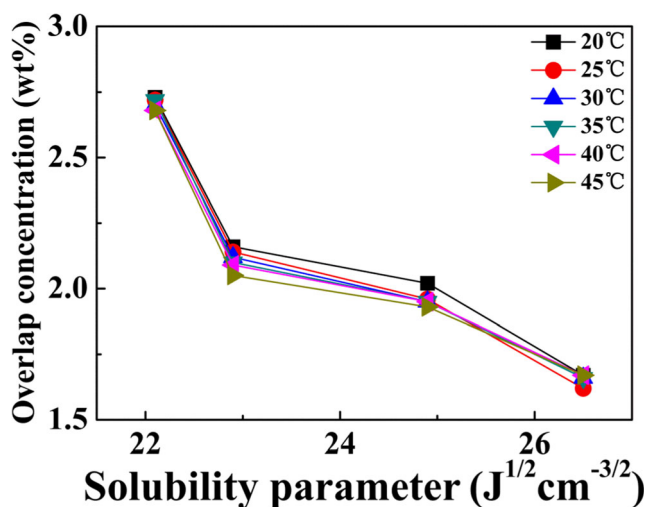


Fig. 10 Relationship between overlap concentration and solubility parameter for 6FDA-TFDB PI sample at different temperatures

TFDB PI solutions. By using rheometer and applying Zimm model (dilute solution), Rouse–Zimm model (semidilute unentangled solution), and Doi–Edwards model (semidilute entangled solution), we obtain the power law exponents and critical concentrations. Results show that all the power law exponents are higher than the theoretical prediction. In dilute solution, power law exponents increase with increased solubility parameter because of the different powers of solvents in screening weak interaction. In semidilute unentangled solution, power law exponents decrease with solubility parameter because the scale of the effective dipole–dipole interaction space becomes small. In semidilute entangled solution, increased solvent solubility parameter results in stronger interaction between the chain segments and the “tube” formed by surrounding polymer chains, which inhibits the reptation of PI chain from the tube and increases the power law exponents. Moreover, the overlap concentration (C^*) and entanglement

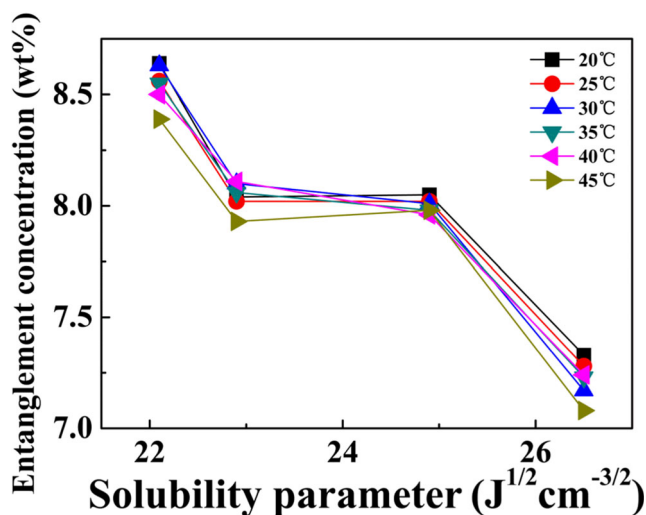


Fig. 11 Relationship between entanglement concentration and solubility parameter for 6FDA-TFDB PI sample at different temperatures

Table 5 Overlap concentration C^* of PI solutions at different temperatures (wt%)

Solvent	20 °C	25 °C	30 °C	35 °C	40 °C	45 °C
DMAc	2.7	2.7	2.7	2.7	2.7	2.7
NMP	2.2	2.1	2.1	2.1	2.1	2.0
DMF	2.0	2.0	2.0	2.0	1.9	1.9
DMSO	1.7	1.6	1.7	1.7	1.7	1.7

Table 6 Entanglement concentration C_e of PI solutions at different temperatures (wt%)

Solvent	20 °C	25 °C	30 °C	35 °C	40 °C	45 °C
DMAc	8.6	8.6	8.6	8.6	8.5	8.4
NMP	8.0	8.0	8.1	8.1	8.1	8.0
DMF	8.1	8.0	8.0	8.0	8.0	8.0
DMSO	7.3	7.3	7.2	7.2	7.2	7.1

concentration (C_e) decrease with increased solubility parameter due to the increased polymer coil radius in solutions.

Acknowledgements We are grateful to the financial supports from National Basic Research Program of China (2014CB643604) and National Natural Science Foundation of China (51173178).

Publisher's Note Springer Nature remains neutral with regard to jurisdictional claims in published maps and institutional affiliations.

References

- Ding M (2007) Isomeric polyimides. *Prog Polym Sci* 32(6):623–668
- Yin C, Dong J, Tan W, Lin J, Chen D (2015) Strain-induced crystallization of polyimide fibers containing 2-(4-aminophenyl)-5-aminobenzimidazole moiety. *Polymer* 75:178–186
- Luo C, Wang X, Wang J, Pan K (2016) One-pot preparation of polyimide/Fe₃O₄ magnetic nanofibers with solvent resistant properties. *Compos Sci Technol* 133:97–103
- Dong J, Yin C, Zhao X, Li Y, Zhang Q (2013) High strength polyimide fibers with functionalized grapheme. *Polymer* 54(23):6415–6424
- Lei X, Qiao M, Tian L, Chen Y, Zhang Q (2016) Tunable permittivity in high-performance hyperbranched polyimide films by adjusting backbone rigidity. *J Phys Chem C* 120(5):2548–2561
- Li B, Pang Y, Fang C, Gao J, Wang X, Zhang C, Liu X (2014) Influence of hydrogen-bonding interaction introduced by filled oligomer on bulk properties of blended polyimide films. *J Appl Polym Sci* 131(13):40498
- Wang L, Hu A, Fan L, Yang S (2014) Structures and properties of closed-cell polyimide rigid foams. *J Appl Polym Sci* 130(5):3282–3291
- Wang H, Wang T, Yang S, Fan L (2013) Preparation of thermal stable porous polyimide membranes by phase inversion process for lithium-ion battery. *Polymer* 54(23):6339–6348

9. Dong Z, Feng T, Zheng C, Li G, Liu F, Qiu X (2016) Mechanical properties of polyimide/multi-walled carbon nanotube composite fibers. *Chin J Polym Sci* 34(11):1386–1395
10. Matsuura T, Hasuda Y, Nishi S, Yamada N (1991) Polyimide derived from 2,2'-bis(trifluoromethyl)-4,4'-diaminobiphenyl. 1. Synthesis and characterization of polyimides prepared with 2,2'-bis(3,4-dicarboxyphenyl)hexafluoropropane dianhydride or pyromellitic dianhydride. *Macromolecules* 24(18):5001–5005
11. Hougham G, Cassidy PE, Johns K, Dsvinson T (2002) *Fluoropolymers 2: properties*. Kluwer Academic Publishers, New York, Boston, Dordrecht, London, Moscow
12. Wang C, Chen W, Xu C, Zhao X, Li J (2016) Fluorinated polyimide/POSS hybrid polymers with high solubility and low dielectric constant. *Chin J Polym Sci* 34(11):1363–1372
13. Siddiq M, Hu H, Ding M, Li B, Wu C (1996) Laser light scattering studies of soluble high-performance polyimides: solution properties and molar mass distributions. *Macromolecules* 29(23):7426–7431
14. Liu G, Qiu X, Bo S, Ji X (2012) Chain conformation and local rigidity of soluble polyimide (II): isomerized polyimides in THF. *Chem Res Chin Univ* 28(2):329–333
15. Liu G, Qiu X, Siddiq M, Bo S, Ji X (2013) Temperature dependence of chain conformation and local rigidity of isomerized polyimides in dimethyl formamide. *Chem Res Chin Univ* 29(5):1022–1028
16. Liu G, Qiu X, Bo S, Ji X (2012) Chain conformation and local rigidity of isomerized polyimides in dimethyl formamide by size exclusion chromatography coupled with multi-detectors. *Chromatographia* 75(1–2):7–15
17. Savitski EP, Li F, Lin SH, McCreight KW, Wu W, Hsieh E, Rapold RF, Leland ME, McIntyre DM, Harris FW, Cheng SZD, Wu C (1997) Investigation of the solution behavior of organo soluble aromatic polyimides. *Int J Polym Anal Charact* 4(2):153–172
18. Zhang E, Dai X, Dong Z, Qiu X, Ji X (2016) Critical concentration and scaling exponents of one soluble polyimide from dilute to semidilute entangled solutions. *Polymer* 84:275–285
19. Zhang E, Chen H, Dai X, Liu X, Yang W, Liu W, Dong Z, Qiu X, Ji X (2017) Influence of molecular weight on scaling exponents and critical concentrations of one soluble 6FDA-TFDB polyimide in solution. *J Polym Res* 24(3):47
20. Zhang E, Dai X, Zhu Y, Chen Q, Sun Z, Qiu X, Ji X (2018) Associating behavior of one polyimide with high molecular weight in solution through a relatively weak interaction. *Polymer* 141:166–174
21. Eom Y, Kim B (2014) Solubility parameter-based analysis of polyacrylonitrile solutions in N,N-dimethylformamide and dimethyl sulfoxide. *Polymer* 55:2570–2577
22. Li W, Hao J, Zhou P, Liu Y, Lu C, Zhang Z (2017) Solvent-solubility-parameter-dependent homogeneity and sol-gel transitions of concentrated polyacrylonitrile solutions. *J Appl Polym Sci* 134:45405
23. Antonietti M, Forster S, Zisenis M (1985) Solution viscosity of polyelectrolyte-surfactant complexes: polyelectrolyte behavior in nonaqueous solvents. *Macromolecules* 28:2270–2275
24. Antoniou E, Buitrago C, Tsianou M, Alexandridis P (2010) Solvent effects on polysaccharide conformation. *Carbohydr Polym* 79:380–390
25. van Krevelen DW, te Nijenhuis K (2010) *Properties of polymers*. Science Press, Beijing, pp 189–225
26. Fedors RF (1974) A method for estimating both the solubility parameters and molar volumes of liquids. *Polym Eng Sci* 14(2):147–154
27. Rubinstein M, Colby RH (2003) *Polymer physics*. Oxford University Press, New York
28. Doi M, Edwards SF (1986) *The theory of polymer dynamics*. Clarendon Press, Oxford
29. Colby RH, Rubinstein M (1990) Two-parameter scaling for polymers in Θ solvents. *Macromolecules* 23(10):2753–2757
30. Bird RB, Curtiss CF, Armstrong RC, Hassager O (1987) *Dynamics of polymeric liquids, vol 1: fluid mechanics* 2nd edn. Wiley, New York
31. Colby RH (2010) Structure and linear viscoelasticity of flexible polymer solutions: comparison of polyelectrolyte and neutral polymer solutions. *Rheol Acta* 49(5):425–442
32. Lu F, Song J, Cheng B, Ji X, Wang L (2013) Viscoelasticity and rheology in the regimes from dilute to concentrated in cellulose 1-ethyl-3-methylimidazolium acetate solutions. *Cellulose* 20:1343–1352
33. Zhu X, Chen X, Saba H, Zhang Y, Wang H (2012) Linear viscoelasticity of poly(acrylonitrile-co-itaconic acid)/1-butyl-3-methylimidazolium chloride extended from dilute to concentrated solutions. *Eur Polym J* 48:597–603
34. Huggins ML (1942) The viscosity of dilute solutions of long-chain molecules. IV dependence on concentration. *J Am Chem Soc* 64: 2716–2718
35. Kraemer EO (1938) Molecular weights of celluloses and cellulose derivatives. *Ind Eng Chem Res* 30(10):1200–1203